HIGH RESOLUTION WEATHER RADAR THROUGH PULSE COMPRESSION

T. A. Alberts[1,*], P. B. Chilson[1], B. L. Cheong[1], R. D. Palmer[1], M. Xue[1,2]

[1] School of Meteorology, University of Oklahoma, Norman, Oklahoma, USA
[2] Center for Analysis and Prediction of Storms, Norman, Oklahoma, USA

Abstract

In order to evaluate pulse compression for use in phased array weather radar systems, modifications to the Time-Series Weather Radar Simulator have been made which incorporate phase-coding into its functionality. This allows for evaluating the performance of various pulse compression schemes under controlled conditions. Barker-coded pulses with matched and mismatched filters were examined in relation to uncoded pulses to determine the performance of the codes with regard to errors in estimating equivalent reflectivity, radial velocity, and spectral width. The 13-bit Barker code with a mismatched filter provided the most accurate estimations due to superior Integrated Sidelobe Level (ISL) suppression capability.

1. INTRODUCTION

With the current trend towards fielding phased array radars that utilize low peak-power T/R modules, methods of recovering potentially lost performance are being examined in greater detail. As such, weather radars that incorporate pulse compression technologies are being analyzed to provide equivalent or better performance to those currently in use.

As a phased array weather radar that is capable of incorporating pulse compression was not available, a simplified framework was created in which the effects of pulse compression on radar returns from meteorological targets could be tested and evaluated. This was completed by leveraging the work by Cheong et al. [2006] and Xue et al. [2003] whereby a weather radar simulator integrates output from the Advanced Regional Prediction System (ARPS) to initialize itself. The ultimate goal of this research is to identify promising waveform and filter combinations that could offset the loss in peak transmitting power in the Multifunction Phased Array Radar being developed through the National Severe Storms Laboratory [Forsyth and et al, 2006] and [Zrnic et al., 2007]. This paper focuses on utilizing Barker codes in the Time-Series Weather Radar Simulator (TSWRS) to baseline the functionality and performance of a limited set of pulse compression schemes.

* *Corresponding author address:* Timothy Alberts, University of Oklahoma, School of Meteorology, 120 David L. Boren Blvd., Rm 4631, Norman, OK 73072-7307; e-mail: talberts@ou.edu

2. BACKGROUND

2.1. Pulse Compression

Pulse compression involves transmitting a coded, wideband signal and compressing the return signal through filtering, which results in increased signal power and enhanced range resolution. Phase codes partition the transmitted pulse into equal segments, or subpulses, and then switch the phase of the signal at specified intervals. In particular, binary phase codes switch the phase between two values, usually 0 and π. The amount of compression possible is equivalent to the time-bandwidth product (BT) of the code, which is the product of the signal bandwidth and signal total duration. Bandwidth of a phase-coded signal is calculated via B=1/τ where τ is taken to be the code subpulse length. The returned signal power increase is proportional to the code length while the range resolution is inversely related to bandwidth as shown in Eq. 1. This implies that decreasing subpulse duration results in a corresponding enhancement in range resolution.

$$\Delta R = \frac{c}{2B} \tag{1}$$

The weakness of such systems is in the creation of range sidelobes which are artifacts produced by the compression process whereby returns from other ranges contaminate the signal at the desired range. The resulting output can cause erroneous estimations of reflectivity, radial velocity, and spectral width. Meteorological applications have the issue of measuring widely distributed phenomena, amplifying the need for adequate ISL suppression. In particular, Barker codes with matched filters have uniformly distributed sidelobes about the mainlobe [Nathanson, 1999] which is higher than the sidelobes by a factor equal to the code length. For example, a 5-bit Barker code in conjunction with a

matched filter will produce a mainlobe 5 times higher than the sidelobes.

Using output of this type we can calculate two metrics that describe the performance of the filtering process. The first metric is the Integrated Sidelobe Level (ISL), as shown in Eq. 2, which compares the total power contained within the sidelobes to the mainlobe. The second metric is the Peak Sidelobe Level (PSL), calculated via Eq. 3, which compares the sizes of the highest sidelobe to the size of the mainlobe. In both of these equations, x_0 refers to the mainlobe magnitude while x_i refers to all other output range sidelobes except the mainlobe. Improvement for both metrics is indicated by a reduction in their respective values. Errors also can be produced by wind velocities within the pulse width but they are of much smaller magnitude than those produced by reflectivity gradients at these transmitting frequencies.

$$ISL = 10 \log \sum_{i=1} \frac{x_i^2}{x_0^2} \tag{2}$$

$$PSL = 10 \log \left[\frac{max(x_i)^2}{x_0^2} \right] \tag{3}$$

2.2. Radar Simulator

Data were generated using the Time-Series Weather Radar Simulator (TSWRS) created by Cheong et al. [2006]. The TSWRS is a 3-dimensional radar simulator consisting of an ensemble of thousands of scatterers placed within the field of view of the virtual radar. It is capable of operating in a dish mode akin to a WSR-88D weather radar as well as in a phased array mode. The meteorological fields used as input to the simulator correspond to output data from the Advanced Regional Prediction System (ARPS) numerical simulation model developed at the Center for the Analysis and Prediction of Storms (CAPS) at OU. The spatial and temporal resolution of the ARPS output used in this study was 25 m and 1 s, respectively. To begin the simulation process, scatterer characteristics are initialized from a known ARPS data set. At the next time step, the scatterer positions are updated according to the wind field as well as their corresponding properties at their new locations. The return signal amplitude and phase from each scatterer is then processed via Monte Carlo integration to calculate time series of the desired meteorological parameters. The test case for all simulations consisted of 99 images representing a small time segment of a tornadic supercell thunderstorm as modeled by the ARPS model. Data were gathered using the dish mode of the TSWRS operating in the S-band at 3.2 GHz. The pulse width was fixed at 1.57μs with a pulse repetition interval of 1 ms, giving an unambiguous range and velocity of 150 km and 23.5 m/s respectively.

2.3. Simulation Procedure

The simulation begins with the input of ARPS data into the TSWRS and the initialization of the scatterer properties. For the cases performed, 30,000 scatterers were used for the standard resolution case while cases incorporating pulse compression increased the number of scatterers that would result in the same average scatterer density of 20 per resolution volume. Next the pulse is propagated throughout the radar field of view on a gate-by-gate basis as shown in Figure 3. The radar then receives the returns from the scatterers and composes the signal. Mathematically, this step can be described by Eq. 4, taken from Mudukutore and Chandrasekar [1998].

$$y[i,j] = \sum_{\forall m+n-1=j} x_i[m,n] \tag{4}$$

After the signal is composed, the simulator decodes the data through the filtering process to produce the data used for estimation of the reflectivity, radial velocity, and spectral width via the autocovariance method. A signal-to-noise ratio of 70 dB was used for all conditions.

3. RESULTS

Using the method described above, Barker codes were incorporated into the simulator for testing the basic functionality of the simulator under controlled conditions. Reflectivity factor, radial velocity, and spectral width were calculated for uncoded and coded pulses at the same range resolution in order to evaluate error performance of the pulse compression scheme. For all cases, the 5-bit Barker code provides a range resolution of 47m while the 13-bit code gives a range resolution of 18m. Figures 2 and 3 illustrate the resolution enhancement obtained by using a 13-bit Barker code with a 25 element mismatched filter. In both figures, plot (a) is the standard 235m resolution case while plots (b) and (c) are 18m resolution cases obtained by an uncoded pulse and a Barker-coded pulse respectively. In these plots, a tornado is located in the upper right corner and is most readily seen by the large gate-to-gate shear in Figure 3 where the large red area on the left is aliased. Plot (c) for each figure has a reduced field of view in terms of minimum and maximum range. The minimum range

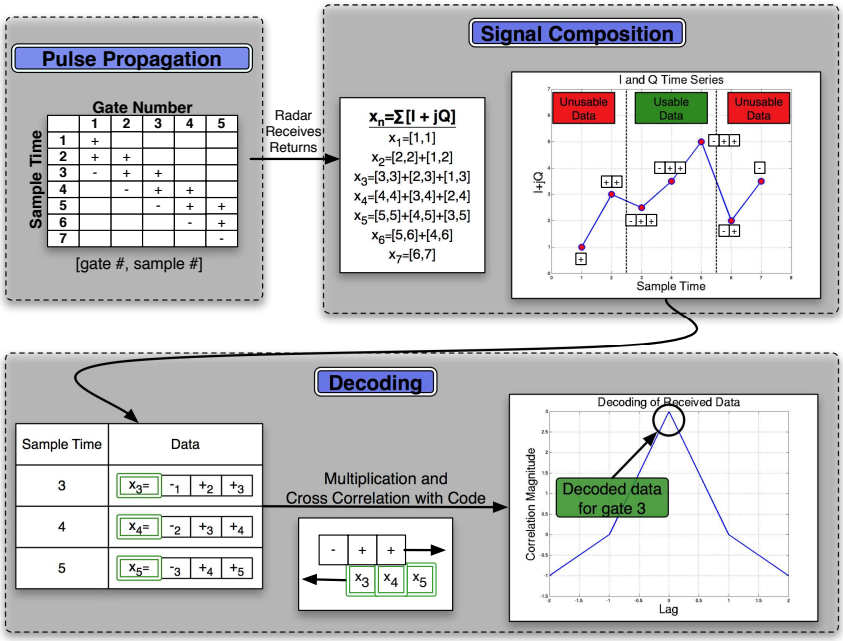

Figure 1: Summary of Simulation Procedure with Matched Filter

increase is due to data needing to fill the mismatched filter which is common to all pulse compression schemes while the reduction of maximum range is the result of the pulse exiting the domain area which again results in a filter that is not filled.

Inspecting plots (b) and (c) in Figures 2 and 3 illustrates that the Barker code process gives reasonable agreement. However, the pulse compression scheme distributes the sharp reflectivity gradient found on the right side of the plot over several range gates. This is a result of the decoding process which can be alleviated by decreasing the ISL as this decreases the amount of interference caused by targets at other ranges. The effect of reducing ISL is illustrated in Figure 4 where the top set of plots use a matched filter for decoding while the bottom plots use a mismatched filter. In all plots, the greatest error coincides with the strong reflectivity gradient around a zonal distance of -9 km but the mismatched filter reduces the mean error from 0.74 dBZ for the matched filter to 0.39 dBZ while also reducing the standard deviation from 2.55 dBZ to 1.81 dBZ. Table 1 summarizes the error performance in terms of mean and standard deviation of various code/filter combinations along the same radial at the same time step. It is shown that using longer codes and mismatched filters drives ISL downward and hence error. This same trend was also seen in errors for velocity and spectral width. Errors due to velocity also occurred but were of significantly smaller magnitude than those resulting from reflectivity.

Table 1: Error Statistics for Barker-coded Pulses

Code	Filter	μ (dBZ)	σ (dBZ)
5-bit	Matched	1.46	3.76
5-bit	Mismatched	0.87	3.52
13-bit	Matched	0.74	2.55
13-bit	Mismatched	0.39	1.81

4. CONCLUSIONS/FUTURE WORK

A successful modification to the TSWRS was presented that produces an increase in range resolution through pulse compression. The simulator currently incorporates Barker phase codes with matched and mismatched filters which show good performance with respect to reflectivity, radial velocity, and spectral width. Large errors did occur where strong reflectivity gradients were present. This highlights the need to explore other code/filter combinations that can suppress ISL even further. This can be achieved by changing code type, code length, filtering method, or any combination of these. However, as code length increases, the Doppler toler-

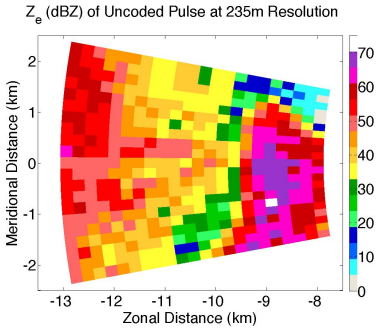

(a) Long Uncoded Pulse, Δr =235m

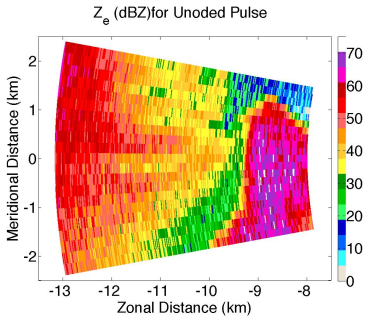

(b) Short Uncoded Pulse, Δr =18m

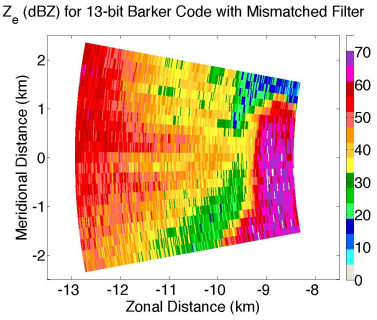

(c) 13-bit Barker-coded Pulse, Δr =18m

Figure 2: Reflectivity Comparison of Uncoded and Coded Pulses.

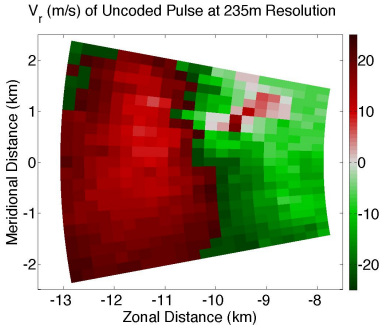

(a) Long Uncoded Pulse, Δr =235m

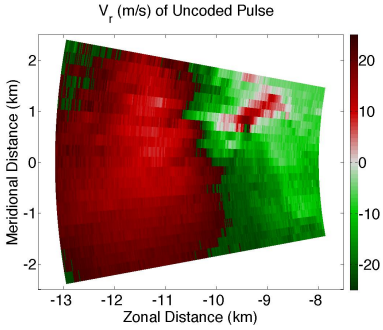

(b) Short Uncoded Pulse, Δr =18m

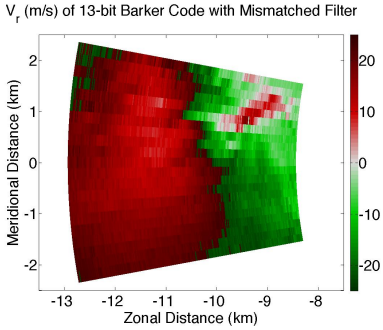

(c) 13-bit Barker-coded Pulse, Δr =18m

Figure 3: Radial Velocity Comparison of Uncoded and Coded Pulses.

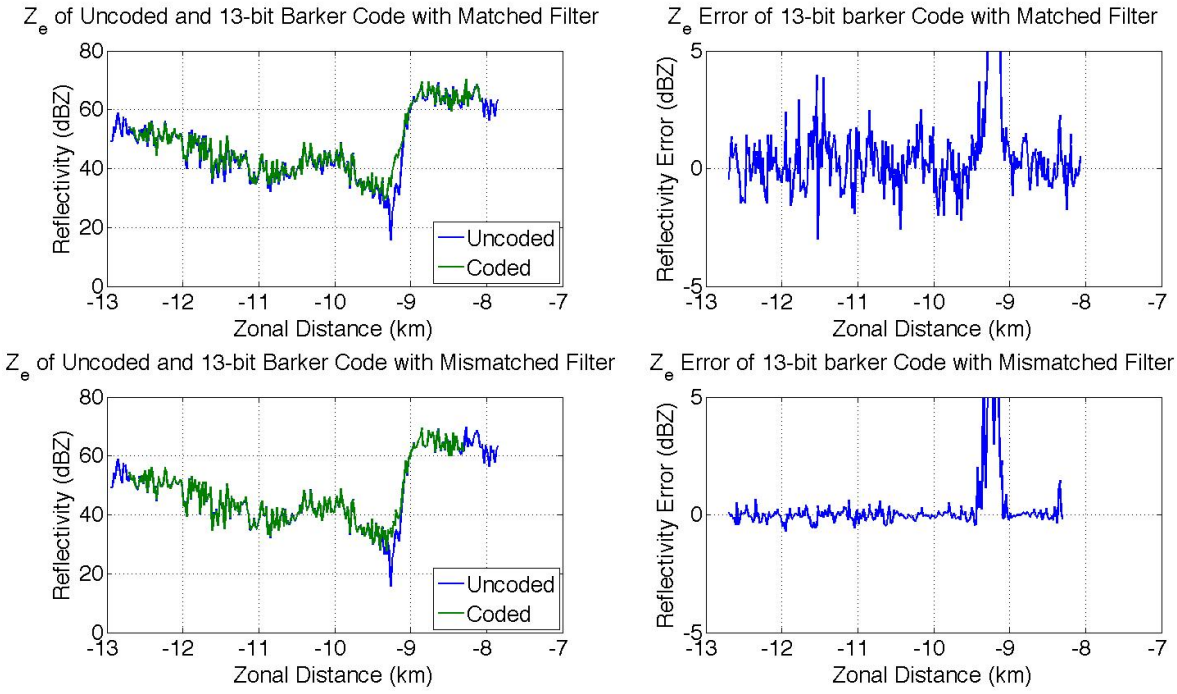

Figure 4: Reflectivity Comparison Along a Radial.

ance of the signal decreases as moving targets can begin to significantly alter the phase of the signal, causing additional errors that need to be mitigated.

Future iterations using this simulator involve testing and evaluation of additional waveform designs and filtering methods. It is also of great interest to expand the domain size beyond what is currently capable. Ideally we would like to recover resolution back to the WSR-88D standard but are currently limited to only 5 km of data. Transmitting a considerably longer pulse would reduce the number of range gates that could be fully decoded to show a valid comparison between an -88D and a phased array radar incorporating pulse compression.

5. ACKNOWLEDGEMENTS

Funding for this work was provided under NOAA cooperative agreement NA17RJ1227. We would also like to thank all those who provided comments to improve this paper.

References

Cheong, B. L., R. D. Palmer, and M. Xue, 2006: A Time-Series Weather Radar Simulator Based on High-Resolution Atmospheric Models. *Submitted to Journal of Atmospheric and Oceanic Technology*.

Forsyth, D. E., and et al, 2006: The National Weather Radar Testbed (Phased-Array). in *32nd Conference on Radar Meteorology*.

Mudukutore, A. S., and V. Chandrasekar, 1998: Pulse Compression for Weather Radars. *IEEE Transactions on Geoscience and Remote Sensing*, **36**(1).

Nathanson, F. E., 1999: *Radar Design Principles*. Prentice-Hall.

Xue, M., D.-H. Wang, J.-D. Gao, K. Brewster, and K. K. Droegemeier, 2003: 2003: The Advanced Regional Prediction System (ARPS), storm-scale numerical weather prediction and data assimilation. *Meteorology and Atmospheric Physics*, **82**, 139–170.

Zrnic, D. S., J. F. Kimpel, D. E. Forsyth, A. Shapiro, G. Crain, R. Ferek, J. Heimmer, W. Benner, T. J. McNellis, and R. J. Vogt, 2007: Agile-beam Phase Array Radar for Weather Observations. *BAMS*, **88**(11), 1753–1766.